

See discussions, stats, and author profiles for this publication at: <https://www.researchgate.net/publication/24199438>

# Intermolecular Vibrational Motions of Solute Molecules Confined in Nonpolar Domains of Ionic Liquids

ARTICLE *in* THE JOURNAL OF PHYSICAL CHEMISTRY B · MAY 2009

Impact Factor: 3.3 · DOI: 10.1021/jp811293n · Source: PubMed

---

CITATIONS

45

---

READS

11

4 AUTHORS, INCLUDING:



E. L. Quitevis

Texas Tech University

76 PUBLICATIONS 2,037 CITATIONS

SEE PROFILE

# Intermolecular Vibrational Motions of Solute Molecules Confined in Nonpolar Domains of Ionic Liquids

Dong Xiao, Larry G. Hines, Jr., Richard A. Bartsch, and Edward L. Quitevis\*

Department of Chemistry and Biochemistry, Texas Tech University, Lubbock, Texas 79409-1061

Received: December 21, 2008; Revised Manuscript Received: February 12, 2009

In this study, we address the following question about the dynamics of solute molecules in ionic liquids (ILs). Are the intermolecular vibrational motions of nonpolar molecules confined in the nonpolar domains formed by tail aggregation in ILs the same as those in an alkane solvent? To address this question, the optical Kerr effect (OKE) spectrum of CS<sub>2</sub> in the IL 1-pentyl-3-methylimidazolium bis(trifluoromethanesulfonyl)amide ([C<sub>5</sub>mim][NTf<sub>2</sub>]) was studied as a function of concentration at 295 K by the use of optical heterodyne-detected Raman-induced Kerr effect spectroscopy. The OKE spectrum broadens and shifts to higher frequency as the CS<sub>2</sub> concentration is decreased from 20 to 10 mol %; at lower concentrations, no further change in the width of the OKE spectrum is observed. Multicomponent line shape analysis of the OKE spectrum of 5 mol % CS<sub>2</sub> in [C<sub>5</sub>mim][NTf<sub>2</sub>] reveals that the CS<sub>2</sub> and [C<sub>5</sub>mim][NTf<sub>2</sub>] contributions to the spectrum are separable and that the CS<sub>2</sub> contribution is similar to the OKE spectrum of 5 mol % CS<sub>2</sub> in *n*-pentane with the spectrum being lower in frequency and narrower than that of neat CS<sub>2</sub>. These results suggest that, at this concentration, CS<sub>2</sub> molecules are isolated from each other and mainly localized in the nonpolar domains of the IL.

## Introduction

Ionic liquids (ILs), which are molten salts with melting points below 373 K, have been in existence for almost a century. However, the past decade has seen an enormous increase in research on ILs,<sup>1,2</sup> driven by the potential applications of ILs in chemical synthesis,<sup>3,4</sup> batteries and solar cells,<sup>5–7</sup> chemical sensors,<sup>8,9</sup> energetic materials,<sup>10</sup> thermal fluids,<sup>11</sup> hydraulic fluids,<sup>12</sup> lubricants,<sup>13</sup> and ionogels.<sup>14</sup> Recently, Raman spectroscopic (linear and nonlinear),<sup>15</sup> X-ray diffraction,<sup>16,17</sup> and diffusion (viscosity, conductivity, NMR)<sup>18</sup> measurements indicate that ILs are spatially heterogeneous at a microscopic level. The most detailed picture of this spatial heterogeneity to date has come from molecular dynamics (MD) simulations of ILs based on the 1-alkyl-3-methylimidazolium cation ([C<sub>*n*</sub>mim]<sup>+</sup>).<sup>19–23</sup> Using a united-atom MD method, Urahata and Ribeiro<sup>19</sup> showed that a low wave vector peak appears in the partial structure factor. They attributed this peak to the occurrence of intermediate range order for C<sub>4</sub> and C<sub>8</sub> but not for shorter chains. Wang and Voth<sup>20,24</sup> used a multiscale coarse-grain MD method to show that heterogeneous domains are formed by the aggregation of alkyl groups for C<sub>4</sub> and longer, with the cation rings and anions homogeneously distributed. Lopes and Padua<sup>21</sup> employed an all-atom MD method to show by color coding of the nonpolar and polar regions that the polar regions are not isolated but are interconnected in such a way as to form a three-dimensional charge-ordered ionic network permeated by nonpolar regions in a manner not unlike that of a swollen gel. Lopes and Padua coined the term “nanostructural organization” to describe this heterogeneity in ILs.

Because of microphase separation between the nonpolar and polar domains in ILs, solute–solvent interactions can be varied

and quite complex, as indicated by MD simulations<sup>23,25</sup> of polar, nonpolar, and associating solutes in ILs. At low concentrations, solute molecules are found in the domains for which the affinity is the greatest. Nonpolar molecules, such as *n*-hexane, tend to reside in the nonpolar domains and are excluded from the ionic networks because of the cohesive energy of the charged groups, whereas associating solutes, such as water, reside mainly in the ionic networks, forming strong hydrogen bonds with the charged part of the ions. On the other hand, dipolar molecules, such as acetonitrile, interact with the nonpolar domains as well as the charged head groups in the ionic networks. At high concentrations, the presence of solute molecules eventually leads to disruption of the nanostructural organization and, in the case of water, to the evolution of micellar structures.<sup>26</sup>

In this Letter, we probe the intermolecular vibrational motions of nonpolar solute molecules dissolved in an IL using the technique of optical heterodyne-detected Raman-induced Kerr effect spectroscopy (OHD-RIKES). OHD-RIKES is a nonlinear optical time-domain technique that measures the collective polarizability anisotropy dynamics of a liquid.<sup>27,28</sup> By use of a Fourier-transform-deconvolution procedure,<sup>29,30</sup> the OHD-RIKES time-domain data can be converted to a reduced spectral density (RSD) or optical Kerr effect (OKE) spectrum, which is directly related to the depolarized Rayleigh/Raman spectrum of the liquid.<sup>31</sup> Because of its ease of use and the high quality of the resultant data, OHD-RIKES has recently become the most common method for studying the low-frequency intermolecular modes of liquids<sup>27,28,32</sup> and, in particular, ILs.<sup>33–43</sup>

We report here a study of the OKE spectrum of CS<sub>2</sub> in the IL 1-pentyl-3-methylimidazolium bis(trifluoromethanesulfonyl)amide ([C<sub>5</sub>mim][NTf<sub>2</sub>]) as a function of the CS<sub>2</sub> concentration. The RSDs are compared to that of a 5 mol % CS<sub>2</sub>/*n*-pentane mixture. The CS<sub>2</sub>/*n*-pentane mixture is an example of a weakly

\* Corresponding author. E-mail: edward.quitevis@ttu.edu.

interacting system where a liquid with a strong optical Kerr response, such as CS<sub>2</sub>, is mixed with a liquid with a weak optical Kerr response, such as a saturated alkane.<sup>44–46</sup> If CS<sub>2</sub> molecules reside in the nonpolar domains, as suggested by MD simulations, the local environment of a CS<sub>2</sub> molecule in [C<sub>5</sub>mim][NTf<sub>2</sub>] should resemble that of CS<sub>2</sub> in *n*-pentane.

## Experimental Section

The synthesis of [C<sub>5</sub>mim][NTf<sub>2</sub>] has been previously described.<sup>47,48</sup> Carbon disulfide and *n*-pentane (Aldrich, spectrochemical grade) were used without further purification. The water content of the freshly synthesized [C<sub>5</sub>mim][NTf<sub>2</sub>] was determined by Karl Fischer titration to be <200 μg/g. The IL was kept in a nitrogen-purged glovebox to prevent the absorption of water. Within the concentration range used in this study, 2.5–20 mol %, CS<sub>2</sub> and [C<sub>5</sub>mim][NTf<sub>2</sub>] were completely miscible and produced mixtures that were optically clear. At 50 mol % and above, the two liquids are immiscible. Samples for the OHD-RIKES measurements were prepared by transferring an aliquot of the liquid to a 2-mm path-length, UV-grade, fused-silica cell (Hellma Cells) with a vacuum stopcock valve. The titanium-sapphire (Ti:S) laser, optical delay line, and pump–probe configuration were the same as previously reported.<sup>33,39,49</sup> The current version of the OHD-RIKES apparatus uses a Coherent Verdi V6 diode-pumped solid-state laser to pump the Ti:S laser. With this pump laser, the Ti:S laser generates 36 fs pulses as determined from the pulse-intensity background-free autocorrelation. The apparatus uses balanced detection and compensates for drift and fluctuations in the laser intensity to increase the signal-to-noise ratio.<sup>27</sup> To minimize the data collection time, scans were carried out in 10 fs steps for time delays between −1 and 4 ps and in 100 fs steps for time delays between 4 and 10 ps. During an OHD-RIKES measurement, a laboratory-built copper cell holder whose temperature was regulated and controlled with a thermoelectric heater/cooler system maintained the temperature at 295 K. The OHD-RIKES data were fit by an empirical decay function. The fit parameters were used to remove the part of the response that decays on a picosecond or longer time scale to yield a reduced OHD-RIKES response. The Fourier transform deconvolution was then applied to the reduced response to obtain the RSD. The current apparatus and the analysis of OHD-RIKES data by the Fourier-transform-deconvolution procedure are described in greater detail in the Supporting Information.

## Results and Discussion

Figure 1 shows the normalized RSDs for 2.5, 5, 10, 15, and 20 mol % CS<sub>2</sub> in [C<sub>5</sub>mim][NTf<sub>2</sub>] and neat CS<sub>2</sub> in the 0–200 cm<sup>−1</sup> range at 295 K with values of the first spectral moment  $\langle\omega\rangle$ , peak frequency  $\omega_{\text{pk}}$ , and full width at half-maximum  $\Delta\omega$  given in Table 1. The smaller peaks in the OKE spectra of the mixtures at 120 and 169 cm<sup>−1</sup> are associated with intramolecular vibrations of the NTf<sub>2</sub><sup>−</sup> ion.<sup>34</sup> As can be seen in Figure 1, upon dilution with [C<sub>5</sub>mim][NTf<sub>2</sub>], the RSD broadens and shifts to higher frequency, which is not unexpected given that the RSD of [C<sub>5</sub>mim][NTf<sub>2</sub>] is higher in frequency and broader ( $\langle\omega\rangle \approx 75$  cm<sup>−1</sup>;  $\Delta\omega \approx 120$  cm<sup>−1</sup>) than that of neat CS<sub>2</sub>. In going from neat CS<sub>2</sub> to 20 mol % CS<sub>2</sub>,  $\langle\omega\rangle$  and  $\Delta\omega$  increase from 43.0 to 58.8 cm<sup>−1</sup> and from 58.8 to 66.4 cm<sup>−1</sup>, respectively. Figure 2 shows that  $\langle\omega\rangle$  increases smoothly with decreasing concentration in the range 2.5–20 mol %. Interestingly,  $\omega_{\text{pk}}$  exhibits the opposite trend in that it decreases with decreasing concentration in this range.

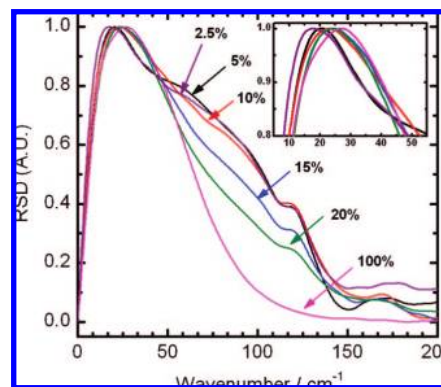


**Figure 1.** Reduced spectral densities of neat CS<sub>2</sub> and CS<sub>2</sub>/[C<sub>5</sub>mim][NTf<sub>2</sub>] mixtures at various CS<sub>2</sub> mole fractions at 295 K. The inset is an enlarged view of the region of the peak in the reduced spectral densities.

**TABLE 1: Spectral Parameters for CS<sub>2</sub>/[C<sub>5</sub>mim][NTf<sub>2</sub>] Mixtures**

mol % CS <sub>2</sub>	$\langle\omega\rangle^a$ (cm <sup>−1</sup> )	$\omega_{\text{pk}}^b$ (cm <sup>−1</sup> )	$\Delta\omega^c$ (cm <sup>−1</sup> )
2.5	66.7	17.8	97.6
5	63.4	20.5	97.9
10	63.3	23.2	96.3
15	60.5	24.4	81.7
20	58.8	24.1	66.4
100	43.0	25.5	58.8

<sup>a</sup> First spectral moment:  $\langle\omega\rangle \equiv \int \omega I_{\text{RSD}}(\omega) d\omega / \int I_{\text{RSD}}(\omega) d\omega$ , where  $I_{\text{RSD}}(\omega)$  is the reduced spectral density with integration limits 0–200 cm<sup>−1</sup>. <sup>b</sup> Peak frequency. <sup>c</sup> Full width at half-maximum.

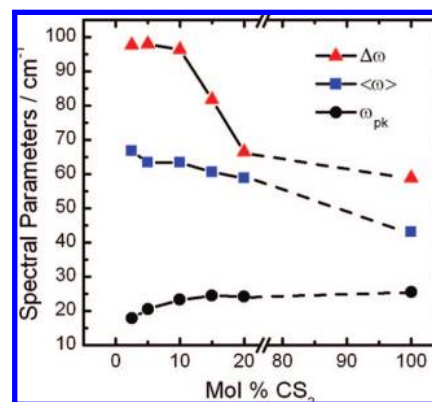


**Figure 2.** Dependence of spectral parameters for CS<sub>2</sub>/[C<sub>5</sub>mim][NTf<sub>2</sub>] mixtures on the concentration of CS<sub>2</sub>.  $\Delta\omega$ , full width at half-maximum;  $\langle\omega\rangle$ , first spectral moment;  $\omega_{\text{pk}}$ , peak frequency. The dashed lines connecting the points at 20 and 100 mol % are only intended to show the change in the spectral parameters in going from neat CS<sub>2</sub> to CS<sub>2</sub>/[C<sub>5</sub>mim][NTf<sub>2</sub>] mixtures. Note that CS<sub>2</sub> and [C<sub>5</sub>mim][NTf<sub>2</sub>] are immiscible for 50 mol % CS<sub>2</sub> and higher concentrations. See Table 1 for values of the spectral parameters.

In contrast, the variation of  $\Delta\omega$  with concentration indicates that there are two distinct concentration regimes (Figure 2): (I) intermediate concentrations between 10 and 20% and (II) low concentrations less than 10 mol %. In regime I, the RSD appears to be largely dominated by CS<sub>2</sub> contributions. Regime II is of particular interest, because the width of the RSD is independent of concentration in this regime. Moreover, the RSDs for 2.5 and 5 mol % mixtures are distinctly narrower in the region of the peak than the RSDs at higher concentrations (Figure 1 inset). This suggests that, within regime II, there may exist secondary effects.

To gain further insight into the intermolecular dynamics of the CS<sub>2</sub>/[C<sub>5</sub>mim][NTf<sub>2</sub>] mixtures in regime II, the OKE spectrum was fit by a sum of two terms

$$I_{\text{mix}}(\omega) = \alpha I_{\text{CS}_2}^{\text{mix}}(\omega) + \beta I_{\text{IL}}^{\text{mix}}(\omega) \quad (1)$$

where  $I_{\text{CS}_2}^{\text{mix}}(\omega)$  is the CS<sub>2</sub> contribution,  $I_{\text{IL}}^{\text{mix}}(\omega)$  is the IL contribution, and  $\alpha$  and  $\beta$  are constants that determine the relative weights of each term. This form of the OKE spectrum makes physical sense, as will be explained below. To facilitate the analysis of the data, the OKE spectra associated with intermolecular vibrational motions of CS<sub>2</sub> were modeled by a two-component line shape function

$$I(\omega) = I_{\text{BL}}(\omega) + I_{\text{G}}(\omega) \quad (2)$$

where the low-frequency component is the Bucaro–Litovitz line shape function

$$I_{\text{BL}}(\omega) = A_{\text{BL}} \omega^a \exp(-\omega/\omega_{\text{BL}}) \quad (3)$$

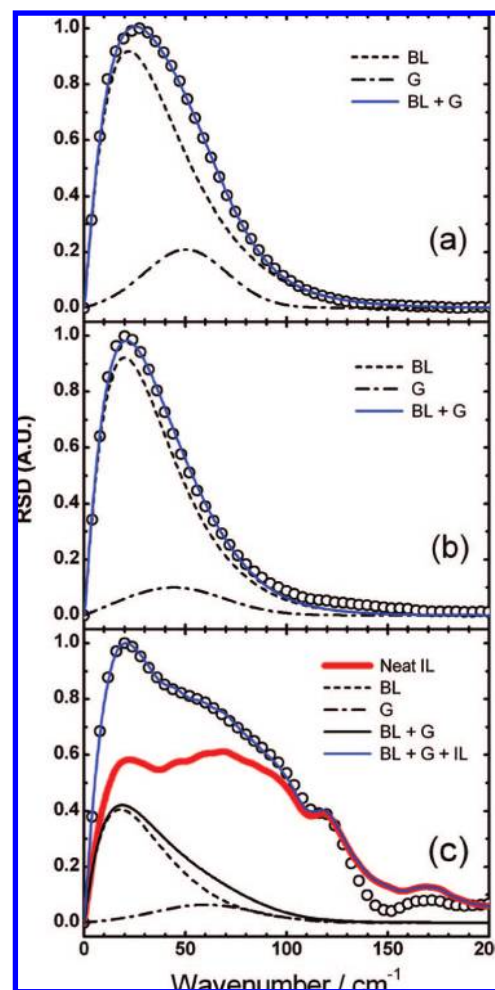
and the high-frequency component is the antisymmetrized Gaussian line shape function

$$I_{\text{G}}(\omega) = A_{\text{G}} \{ \exp[-(\omega - \omega_{\text{G}})^2/2\varepsilon^2] - \exp[-(\omega + \omega_{\text{G}})^2/2\varepsilon^2] \} \quad (4)$$

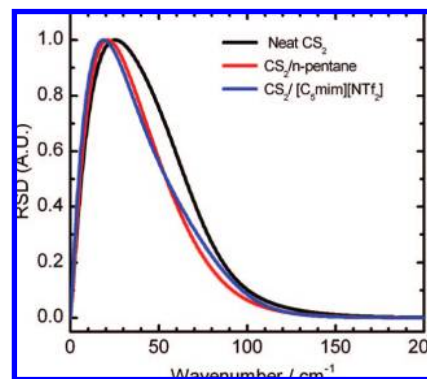
Figures 3a and b show the RSDs of neat CS<sub>2</sub> and the 5 mol % CS<sub>2</sub>/n-pentane mixture, respectively, along with fits of the two-component line shape function (eq 2) over the frequency range 0–200 cm<sup>-1</sup>. In the case of neat CS<sub>2</sub>, there is good agreement between the fit and the RSD. In the case of the CS<sub>2</sub>/n-pentane mixture, eq 2 provides a good fit of the main band in the 0–100 cm<sup>-1</sup> region but slightly underestimates the high-frequency tail in the 100–200 cm<sup>-1</sup> region. These results indicate the use of the two-component line shape function should provide a reasonable quantitative description of the CS<sub>2</sub> contribution of the OKE spectrum of the CS<sub>2</sub>/[C<sub>5</sub>mim][NTf<sub>2</sub>] mixture.

Figure 3c shows the RSD of the 5 mol % CS<sub>2</sub>/[C<sub>5</sub>mim][NTf<sub>2</sub>] mixture, along with the fit of eq 1, where  $I_{\text{CS}_2}^{\text{mix}}(\omega)$  is given by a normalized two-component line shape function in eq 2 and  $I_{\text{IL}}^{\text{mix}}(\omega)$  by the normalized RSD of neat [C<sub>5</sub>mim][NTf<sub>2</sub>]. Excellent agreement between the fit of eq 1 and the experimental RSD is obtained for  $\alpha = 0.41$  and  $\beta = 0.59$  over most of the given frequency range, with slight deviations occurring in the high-frequency tail. (Note that the ratio of the coefficients  $\alpha/\beta$  is not equal to the ratio of mole fractions  $X_{\text{CS}_2}/(1 - X_{\text{CS}_2})$ , because the polarizability anisotropies of CS<sub>2</sub> and the IL are not the same.) In order to focus on the intermolecular dynamics of CS<sub>2</sub> in these three systems, the optical Kerr spectral components arising from the sum of the Bucaro–Litovitz and antisymmetrized Gaussian functions are shown in Figure 4. Fit parameters for the two-component line shape function are listed in Table 2.

The CS<sub>2</sub> contribution to the RSD of the CS<sub>2</sub>/[C<sub>5</sub>mim][NTf<sub>2</sub>] mixture is strikingly similar to the RSD of the CS<sub>2</sub>/n-pentane mixture, as can be seen in Figure 4 and as evidenced by the peak frequency and fwhm:  $\omega_{\text{pk}} = 19.0$  cm<sup>-1</sup> and  $\Delta\omega = 49.7$  cm<sup>-1</sup> for  $I_{\text{CS}_2}^{\text{mix}}(\omega)$  and  $\omega_{\text{pk}} = 21.0$  cm<sup>-1</sup> and  $\Delta\omega = 48.6$  cm<sup>-1</sup> for the RSD of the CS<sub>2</sub>/n-pentane mixture. One might argue



**Figure 3.** Reduced spectral density of (a) neat CS<sub>2</sub> (points) with fit of the two-component line shape function (eq 2), (b) 5 mol % CS<sub>2</sub>/n-pentane mixture (points) with fit of the two-component line shape function (eq 2), and (c) 5 mol % CS<sub>2</sub>/[C<sub>5</sub>mim][NTf<sub>2</sub>] with fit of the model line shape function (eq 1). The component bands used in the fit of the reduced spectral densities are also shown. BL, Bucaro–Litovitz line shape function; G, antisymmetrized Gaussian line shape function; IL, reduced spectral density of neat [C<sub>5</sub>mim][NTf<sub>2</sub>].



**Figure 4.** Spectra of the intermolecular vibrations of CS<sub>2</sub> obtained from the sum of the Bucaro–Litovitz and antisymmetrized Gaussian functions (eqs 2–4) corresponding to the reduced spectral densities in Figure 2. See Table 2 for fit parameters.

that this comparison should be made for solutions with the same volume fraction. If we assume additivity of volumes, then a 5 mol % solution of CS<sub>2</sub> in [C<sub>5</sub>mim][NTf<sub>2</sub>] is equivalent to a 1.1 vol % solution, and a 5 mol % solution of CS<sub>2</sub> in n-pentane is equivalent to a 2.7 vol % solution. Thus, instead of using a 5



**TABLE 2: Fit Parameters for Intermolecular Spectra of Neat CS<sub>2</sub>, CS<sub>2</sub> in *n*-Pentane, and CS<sub>2</sub> in [C<sub>5</sub>mim][NTf<sub>2</sub>]**

liquid	$\omega_{\text{pk}}^c$ (cm <sup>-1</sup> )	$\Delta\omega^d$ (cm <sup>-1</sup> )	Bucaro–Litovitz <sup>a</sup>			antisymmetrized Gaussian <sup>b</sup>		
			$A_{\text{BL}}$	$a$	$\omega_{\text{BL}}$ (cm <sup>-1</sup> )	$A_{\text{G}}$	$\omega_{\text{G}}$ (cm <sup>-1</sup> )	$\varepsilon$ (cm <sup>-1</sup> )
neat CS <sub>2</sub>	25.5	58.8	0.084	1.14	19.4	0.21	50.2	20.3
CS <sub>2</sub> / <i>n</i> -pentane <sup>e</sup>	21.0	48.6	0.087	1.18	16.9	0.1	44.0	25.0
CS <sub>2</sub> /[C <sub>5</sub> mim][NTf <sub>2</sub> ] <sup>e</sup>	19.0	49.7	0.12	1.10	16.4	0.15	60.0	25.0

<sup>a</sup> See eq 3 for definition of parameters. <sup>b</sup> See eq 4 for definition of parameters. <sup>c</sup> Peak frequency of the two-component line shape function (eq 2). <sup>d</sup> Full width at half-maximum of the two-component line shape function (eq 2). <sup>e</sup> 5 mol % mixture.

mol % CS<sub>2</sub>/pentane mixture, we should have used a 2 mol % CS<sub>2</sub>/pentane mixture, which is equivalent to a 1.1 vol % solution. However, at these low concentrations, it should not matter whether a 2 or 5 mol % CS<sub>2</sub>/*n*-pentane mixture is used, because the RSDs for CS<sub>2</sub>/*n*-pentane mixtures are independent of concentration for volume fractions less than 20%.<sup>50</sup>

A key feature in the intermolecular dynamics of CS<sub>2</sub> is the shift in the peak frequency of the OKE spectrum from 25.5 to 21.0 cm<sup>-1</sup> and a decrease in the fwhm from 58.8 to 48.6 cm<sup>-1</sup> upon dilution in *n*-pentane. The similarity of  $I_{\text{CS}_2}^{\text{mix}}(\omega)$  to the RSD of the CS<sub>2</sub>/*n*-pentane mixture indicates that the mechanism giving rise to the shift toward lower frequency and narrowing for CS<sub>2</sub> in *n*-pentane must be the same for CS<sub>2</sub> confined in the nonpolar domains of [C<sub>5</sub>mim][NTf<sub>2</sub>]. The shift toward lower frequency and narrowing upon dilution are commonly observed in the OKE spectra of weakly interacting systems.<sup>44–46,50,51</sup> The origin of this dilution effect is controversial.<sup>50,51</sup> Recent experiments, however, strongly support the idea that the effect is due to softening of the intermolecular potential upon dilution.<sup>52,53</sup> For rather weakly interacting molecules such as CS<sub>2</sub> and *n*-pentane, one expects mixing to largely be determined by entropy. Therefore, in dilute solution, a CS<sub>2</sub> molecule has a higher probability of interacting with an *n*-pentane molecule than with another CS<sub>2</sub> molecule. Because CS<sub>2</sub>–*n*-pentane interactions are weaker than CS<sub>2</sub>–CS<sub>2</sub> interactions, the average intermolecular potential that a CS<sub>2</sub> molecule sees in a dilute *n*-pentane solution will be weaker than in neat CS<sub>2</sub>.

At a CS<sub>2</sub> concentration of 5 mol %, the population of CS<sub>2</sub> molecules in the nonpolar domains of the IL is low. To see this, we make use of recent small- and wide-angle X-ray scattering measurements on [C<sub>5</sub>mim][NTf<sub>2</sub>] at 298 K that indicate a spatial correlation length of  $D = 11.4$  Å associated with the size of the structural heterogeneities in the IL.<sup>54</sup> If we assume a spherical shape for the structural heterogeneities, then  $D$  corresponds to the average size of the domains, which includes the alkyl tail domain size and thickness of the charged shell.<sup>17</sup> On the basis of the density  $\rho = 1.4042$  g/cm<sup>3</sup> for the 5 mol % CS<sub>2</sub>/[C<sub>5</sub>mim][NTf<sub>2</sub>] mixture, we calculate the concentration of CS<sub>2</sub> in the IL solution to be  $1.0 \times 10^{20}$  molecules/cm<sup>3</sup>. At this concentration, CS<sub>2</sub> molecules are isolated from each and separated by an average distance of  $\sim 20$  Å. The distance between CS<sub>2</sub> molecules is roughly twice the correlation length of the heterogeneities in the IL, which suggests that the nonpolar domains are less than singly occupied.

A CS<sub>2</sub> molecule in a nonpolar domain is within  $\sim 5$  Å of the ionic networks where the imidazolium rings are located. If there is equal probability for finding CS<sub>2</sub> molecules anywhere in the domains, then a fraction of the CS<sub>2</sub> molecules should be near the interfacial region (i.e., domain wall) separating the nonpolar domain from the ionic network. This scenario would give rise to interaction-induced (I–I) contributions to the many-body polarizability that involve coupling of the CS<sub>2</sub> molecules and the imidazolium rings in the ionic network. The presence of such terms would lead to nonadditivity of the OKE spectra of

the mixture, contrary to the results of our analysis, which are based on the assumption of separability of the intermolecular modes of CS<sub>2</sub> and the IL, as stated in eq 1. Therefore, the only plausible explanation for the additivity of the OKE spectra, as well as for the similarity of the CS<sub>2</sub> contribution to the RSD of the CS<sub>2</sub>/[C<sub>5</sub>mim][NTf<sub>2</sub>] mixture and the RSD of the CS<sub>2</sub>/*n*-pentane mixture, is that the CS<sub>2</sub> molecules mainly reside in the interior of the nonpolar domains and not near the domain walls.

In conclusion, this study has shown that, on the basis of a comparison of the OKE spectra of 5 mol % CS<sub>2</sub>/[C<sub>5</sub>mim][NTf<sub>2</sub>] and 5 mol % CS<sub>2</sub>/*n*-pentane solutions, the intermolecular vibrational motions of CS<sub>2</sub> in the IL are the same as that of CS<sub>2</sub> in *n*-pentane. The results in this study are consistent with the MD simulations that show segregation of polar and nonpolar domains in imidazolium-based ILs and the solvation of nonpolar molecules in the nonpolar domains. A complete understanding of the intermolecular dynamics of nonpolar solute molecules in ILs will require analysis of OKE spectra at higher concentrations. This will be done in a subsequent paper. To our knowledge, this is the first study of the intermolecular dynamics of solute molecules confined in the nonpolar domains of ILs. This work opens up opportunities for examining the intermolecular vibrational motions of solute molecules in ILs from the perspective of soft spatial confinement. By varying the alkyl chain length, the effect of domain size on the solute intermolecular dynamics can be studied. By varying the cohesive energy of the ionic networks by changing the size of the anion, the effect of the stiffness of the domain walls can be studied. Finally, OHD-RIKES measurements on dipolar molecules, such as acetonitrile, in ILs will provide insights into solute intermolecular dynamics at the interface of the nonpolar domains and ionic networks. These studies are currently being pursued in our laboratories.

**Acknowledgment.** This research was supported by grants from the National Science Foundation (CHE-0718678) and the American Chemical Society Petroleum Research Fund (47615-AC6) to E.L.Q. and from The Welch Foundation (D-0775) to R.A.B. We thank Ali Mohammed for helping with the OKE measurements.

**Supporting Information Available:** Description of the OHD-RIKES apparatus, OHD-RIKES signals, and the Fourier-transform-deconvolution procedure. This material is available free of charge via the Internet at <http://pubs.acs.org>.

## References and Notes

- (1) *Ionic Liquids IIIA: Fundamentals, Progress, Challenges, and Opportunities. Properties and Structure*; Rodgers, R. D., Seddon, K. R., Eds.; ACS Symposium Series 901; American Chemical Society: Washington, DC, 2005.
- (2) *Ionic Liquids IIIB: Fundamentals, Progress, Challenges, and Opportunities. Transformations and Processes*; Rodgers, R. D., Seddon, K. R., Eds.; ACS Symposium Series 902; American Chemical Society: Washington, DC, 2005.

- (3) Welton, T. *Chem. Rev.* **1999**, 99, 2071.
- (4) Wasserscheid, P.; Keim, W. *Angew. Chem., Int. Ed.* **2000**, 39, 3772.
- (5) Nakagawa, H.; Izuchi, S.; Kuwana, K.; Nukuda, T.; Aihara, Y. *J. Electrochem. Soc.* **2003**, 150, A695.
- (6) Peng, W.; Zakeeruddin, S. M.; Ivan, E.; Gratzel, M. *Chem. Commun.* **2002**, 2972.
- (7) Fredlin, K.; Gorlov, M.; Pettersson, H.; Hagfeldt, A.; Kloo, L.; Boschloo, G. *J. Phys. Chem. C* **2007**, 111, 13261.
- (8) Jin, X.; Yu, L.; Garcia, D.; Ren, R. X.; Zeng, X. *Anal. Chem.* **2006**, 78, 6980.
- (9) Wei, D.; Ivaska, A. *Anal. Chim. Acta* **2008**, 607, 126.
- (10) Smiglak, M.; Metlen, A.; Rodger, R. D. *Acc. Chem. Res.* **2007**, 40, 1182.
- (11) Van Valkenburg, M. E.; Vaughn, R. L.; Williams, M.; Wilkes, J. S. *Thermochim. Acta* **2005**, 425, 181.
- (12) Gu, W.; Chen, H.; Tung, Y.-C.; Meiners, J.-C.; Takayama, S. *Appl. Phys. Lett.* **2003**, 90, 033505/1.
- (13) Sanes, J.; F.-J., C.; Bermudez, M.-D.; Martinez-Nicolas, G. *Tribol. Lett.* **2006**, 21, 121.
- (14) Le Bideau, J.; Gaveau, P.; Bellayer, S.; Neouze, M.-A.; Vioux, A. *Phys. Chem. Chem. Phys.* **2007**, 9, 5419.
- (15) Iwata, K.; Okajima, H.; Saha, S.; Hamaguchi, H.-O. *Acc. Chem. Res.* **2007**, 40, 1174.
- (16) Triolo, A.; Russina, O.; Bleif, H.-J.; Di Cola, E. *J. Phys. Chem. B* **2007**, 111, 4641.
- (17) Triolo, A.; Russina, O.; Fazio, B.; Triolo, R.; Di Cola, E. *Chem. Phys. Lett.* **2008**, 457, 362.
- (18) Tokuda, H.; Hayamizu, K.; Ishii, K.; Susan, M. A. B.; Watanabe, M. *J. Phys. Chem. B* **2005**, 109, 6103.
- (19) Urahata, S. M.; Ribeiro, M. C. C. *J. Chem. Phys.* **2004**, 120, 1855.
- (20) Wang, Y.; Voth, G. A. *J. Am. Chem. Soc.* **2005**, 127, 12192.
- (21) Lopes, J. N. A. C.; Padua, A. A. H. *J. Phys. Chem. B* **2006**, 110, 3330.
- (22) Wang, Y.; Voth, G. A. *J. Phys. Chem. B* **2006**, 110, 18601.
- (23) Lopes, J. N. A. C.; Gomes, M. F. C.; Padua, A. A. H. *J. Phys. Chem. B* **2006**, 110, 16816.
- (24) Wang, Y.; Yan, T.; Voth, G. A. *Acc. Chem. Res.* **2007**, 40, 1193.
- (25) Padua, A. A. H.; Gomes, M. F. C.; Lopes, J. N. A. C. *Acc. Chem. Res.* **2007**, 40, 1087.
- (26) Jiang, W.; Wang, Y.; Voth, G. A. *J. Phys. Chem. B* **2007**, 111, 4812.
- (27) Fourkas, J. T. In *Ultrafast Infrared and Raman Spectroscopy*; Fayer, M. D., Ed.; Marcel Dekker, Inc.: New York, 2001.
- (28) Smith, N.; Meech, S. R. *Int. Rev. Phys. Chem.* **2002**, 21, 75.
- (29) McMorow, D. *Opt. Commun.* **1991**, 86, 236.
- (30) McMorow, D.; Lotshaw, W. T. *J. Phys. Chem.* **1991**, 95, 10395.
- (31) Kinoshita, S.; Kai, Y.; Yamaguchi, M.; Yagi, T. *Phys. Rev. Lett.* **1995**, 75, 148.
- (32) Hunt, N. T.; Jaye, A. A.; Meech, S. R. *Phys. Chem. Chem. Phys.* **2007**, 9, 2167.
- (33) Hyun, B. R.; Dzyuba, S. V.; Bartsch, R. A.; Quitevis, E. L. *J. Phys. Chem. A* **2002**, 106, 7579.
- (34) Giraud, G.; Gordon, C. M.; Dunkin, I. R.; Wynne, K. *J. Chem. Phys.* **2003**, 119, 464.
- (35) Rajian, J. R.; Li, S.; Bartsch, R. A.; Quitevis, E. L. *Chem. Phys. Lett.* **2004**, 393, 372.
- (36) Shirota, H.; Funston, A. M.; Wishart, J. F.; Castner, E. W., Jr. *J. Chem. Phys.* **2005**, 122, 184512(1).
- (37) Shirota, H.; Castner, E. W., Jr. *J. Phys. Chem. A* **2005**, 109, 9388.
- (38) Shirota, H.; Castner, E. W., Jr. *J. Phys. Chem. B* **2005**, 109, 21576.
- (39) Xiao, D.; Rajian, J. R.; Li, S.; Bartsch, R. A.; Quitevis, E. L. *J. Phys. Chem. B* **2006**, 110, 16174.
- (40) Xiao, D.; Rajian, J. R.; Cady, A.; Li, S.; Bartsch, R. A.; Quitevis, E. L. *J. Phys. Chem. B* **2007**, 111, 4669.
- (41) Shirota, H.; Wishart, J. F.; Castner, E. W. *J. Phys. Chem. B* **2007**, 111, 4819.
- (42) Castner Jr, E. W.; Wishart, J. F.; Shirota, H. *Acc. Chem. Res.* **2007**, 40, 1217.
- (43) Xiao, D.; Rajian, J. R.; Hines, L.; Li, S.; Bartsch, R. A.; Quitevis, E. L. *J. Phys. Chem. B* **2008**, 112, 13316.
- (44) Kalpouzos, C.; McMorow, D.; Lotshaw, W. T.; Kenney-Wallace, G. A. *Chem. Phys. Lett.* **1988**, 150, 138.
- (45) Kalpouzos, C.; McMorow, D.; Lotshaw, W. T.; Kenney-Wallace, G. A. *Chem. Phys. Lett.* **1989**, 155, 240.
- (46) McMorow, D.; Thant, N.; Melinger, J. S.; Kim, S. K.; Lotshaw, W. T. *J. Phys. Chem.* **1996**, 100, 10389.
- (47) Dzyuba, S. V.; Bartsch, R. A. *J. Heterocycl. Chem.* **2001**, 38, 265.
- (48) Dzyuba, S. V.; Bartsch, R. A. *ChemPhysChem* **2002**, 3, 161.
- (49) Hyun, B. R.; Quitevis, E. L. *Chem. Phys. Lett.* **2003**, 370, 725.
- (50) Steffen, T.; Meinders, N. A. C. M.; Duppen, K. *J. Phys. Chem. A* **1998**, 102, 4213.
- (51) McMorow, D.; Thant, N.; Kleinman, V.; Melinger, J. S.; Lotshaw, W. T. *J. Phys. Chem. A* **2001**, 105, 7960.
- (52) Scodinu, A.; Fourkas, J. T. *J. Phys. Chem. B* **2003**, 107, 44.
- (53) Zhong, Q.; Fourkas, J. T. *J. Phys. Chem. B* **2008**, 112, 15529.
- (54) Xiao, D.; Hines, L.; Li, S.; Bartsch, R. A.; Quitevis, E. L.; Russina, O.; Triolo, A. *J. Phys. Chem. B*. In press.

JP811293N